Normalization-Based Approach to Electric Motor BVR Related Capacitances Computation

J. Ahola[†], A. Muetze[‡], M. Niemelä[†], and A. Romanenko[†]

[†]Department of Electrical Engineering
Lappeenranta University of Technology
P.O. Box 53851 Lappeenranta
Finland

[‡]Electric Drives and Machines Institute
Graz University of Technology
Inffeldgasse 18, A-8010 Graz
Austria

***Abstract*—Electrical discharge machining (EDM) bearing currents that may occur within electric machines of variable-speed-driven motor systems have been recognized for a long time. One important factor of influence, the capacitive voltage divider "bearing-voltage-ratio" BVR of the machine strongly depends on the rotor-to-frame and the stator winding-to-rotor capacitances which are, in turn, affected by the design of the machine's stator slot. This paper presents an approach to improve the accuracy with which these capacitances can be estimated. It is based on the well-known plate capacitance equation which is then corrected by normalization functions. The functions are defined by extensive parameter studies using electrostatic FEM simulations. The final expressions not only allow relatively accurately predicting the stator-winding-to-rotor and rotor-to-frame capacitances. They are also easily applicable, so as to, for example, easily study the sensitivity of the BVR towards changes of the different stator slot parameters.**

Keywords—bearing currents, electric machine, modelling, variable speed drive.

I. INTRODUCTION

THE phenomenon of inverter-induced bearing currents that may cause unexpected breakdowns in variable-speed-drive (VSD) systems has been well-recognized and widely studied, e.g., [1]-[6]. Different types of bearing currents, with different cause-effect chains, can be distinguished, electric discharge machining (EDM) bearing currents being one of them. The main causes of EDM currents have been understood and modeling approaches at different system levels have been proposed. However, techniques to correctly determine the model parameters are still highly needed. This paper focuses on the improvement of two parameters that centrally influence the so-called "bearing-voltage-ratio" (BVR) that describes the ratio of the voltage occurring across the bearing and the common mode voltage at the stator terminals. The BVR is, next to the speed the machine is operating at, the most important parameter related to the electric machine itself that determines the occurrence of EDM bearing currents and their character (notably amplitude). Such EDM currents are considered to be notably prevalent and harmful in physically relatively small electrical machines.

The BVR is mainly determined by the capacitances between the rotor and the frame, C_{rf}, and the winding and the rotor, C_{wr}. This paper extends previous works on the physics based computation of these two capacitances. As a matter of fact, the stator slot dimensions significantly affect the values of these two capacitances. In contrast to the capacitances of the bearings, which depend on the operating point of the machine (notably its load, temperature, and rotational speed [7]-[9]), these two capacitances are determined within the overall design process of the electric machine. Certainly, many factors will eventually determine the design of the slots and their openings. However, availability of advanced modeling techniques, such as those proposed in this paper, will eventually allow considering also the resulting BVR of the final machine design within the design process.

The starting point for the proposed physics-based approach to calculate the stator-winding-to-rotor and the rotor-to-frame capacitances is the well-known analytic parallel-plate capacitance equation. It has also previously been proposed in [5] and [10] for the calculation of the stator-winding-to-rotor capacitance. In these works, the rotor-to-frame capacitance is calculated by a cylindrical capacitor approximation, in [10], the established Carter factor, k_c, is used additionally to consider the effect of the slot openings on the electric field.

In contrast to the previous work, we propose to consider the non-idealities due to the nonhomogeneous electric field around the stator slot opening, both in the calculation of the rotor-to-frame and the stator-winding-to-rotor capacitance, by empirically obtained normalization functions, $k_{rf} = f(d_{ag}/w_s)$ and $k_{wr} = f(d_{tot}/w_{so})$, respectively, where d_{ag} is the air gap, w_s the stator tooth width, d_{tot} the distance of the stator winding from the rotor surface and w_{so} is the slot opening width. These functions are defined by extensive parameter studies using electrostatic FEM simulation to analyze different stator slot designs. The theoretical work is verified experimentally for electric machines of different size. The final expressions not only allow relatively accurately predicting the stator-winding-to-rotor and the rotor-to-frame capacitances, but also easily studying, e.g., the sensitivity of the BVR towards changes of the different parameters of the stator slot.

978-1-5386-1180-7/18/$31.00 ©2018 IEEE

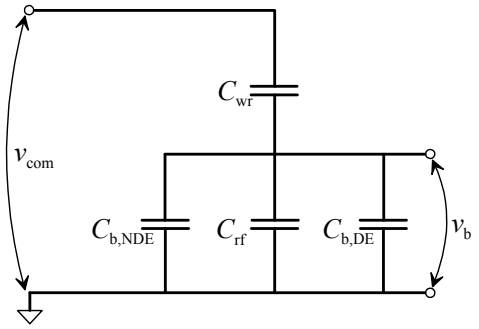

Figure 1. Established equivalent circuit for the determination of the bearing-voltage-ratio (BVR) in electric machines.

The two capacitances considered, the stator-winding-to-rotor capacitance, C_{wr}, and the rotor-to-frame capacitance, C_{rf}, are those most relevant for the value of the BVR. The determination of the bearing capacitances and/or improvements of the BVR model are beyond the scope of this paper.

The paper is organized as follows. The following Section II shortly presents the BVR model, as it is commonly used today, and identifies the important role of the stator-winding-to-rotor capacitance, C_{wr}, and the rotor-to-frame capacitance, C_{rf} with respect to the BVR. Sections III and IV review the previously proposed models to compute these capacitances and discuss the here presented new normalization function based approaches, for each of the two capacitances respectively. Section V presents the results of the FEM analysis and the derivation of the normalization functions, both from simulated and from measured data. Section VI describes the experimentally based part of the research program. Finally, the paper closes with some conclusions presented in Section VII.

II. Bearing-Voltage-Ratio

Per its definition, the BVR determines the ratio of the voltage across the bearing, v_b, and the common mode voltage at the stator terminals, v_{com}, as it results from the capacitive voltage divider given by capacitances within the electric machine [5]. Figure 1 shows the BVR equivalent circuit. It consists of the stator-winding-to-rotor capacitance, C_{wr}, the rotor-to-frame capacitance, C_{rf}, and the two bearing capacitances both on the drive-end, $C_{b,DE}$, and on the non-drive end, $C_{b,NDE}$. Then, the BVR is given by

$$\mathrm{BVR} = \frac{v_b}{v_{com}} = \frac{C_{wr}}{C_{wr} + C_{rf} + C_{b,DE} + C_{b,NDE}} . \quad (1)$$

The stator windings in the slots and the rotor surface form the stator-winding-to-rotor capacitance C_{wr}. The distance between the two plates of the capacitance is rather long and the width is small, when compared with those of the rotor-to-frame capacitance C_{rf}. Here, the rather wide teeth including their tips face the rotor surface at very small distance. As per [10], the orders of magnitudes of the three capacitances that form the BVR relate as follows

$$C_{wf} = \left(\frac{1}{10} \ldots \frac{1}{20}\right) C_{rf} , \quad (2)$$

$$C_{wf} \approx C_b . \quad (3)$$

With the proportions of C_{rf}, C_{wr} and C_b given in (2) and (3), the effect of the bearing capacitances C_b on the BVR is small. For example, for $C_{wr} = C_b = 1/15\ C_{rf}$, (1) gives BVR = 5.6 %. By neglecting the bearing capacitances C_b, we obtain BVR = 6.3 %. Considering the degree to which the BVR can be determined because of the uncertainty inherent in the estimation of the values of the capacitances C_{rf} and C_{wr}, this difference is considered acceptable. Non-zero bearing capacitances always reduce the value of the BVR.

III. Rotor-to-Frame Capacitance Computation

A. Previously Proposed Approach

The rotor-to-frame capacitance C_{rf} is formed between the stator iron and rotor surfaces. As per [5] and [10], the stator and the rotor surfaces may be assumed to form a coaxial air-insulated capacitor, in which the electrodes are separated by the machine air gap, d_{ag}. Since the air-gap is rather small when compared to the rotor diameter, d_r, $d_{ag} << d_r$, the capacitor can be simplified as an air-insulated plate capacitor with the length of the stator stack, l_s, and permittivity of vacuum $\varepsilon_0 = 8.854 \cdot 10^{-12}$ [F/m]. In [10], the effect of the stator slot openings is taken into account by the established Carter coefficient k_c, which is derived via conformal mapping. With these assumptions, C_{rf} is calculated as

$$C_{rf} = \varepsilon_0 \pi \frac{d_r l_s}{k_c d_{ag}} . \quad (4)$$

While the cylindrical capacitor approximation and application of k_c are justified, (4) does not explicitly consider the relation between the width of the stator tooth, w_s, and of the machine's air gap, d_{ag}, instead, this ratio is considered implicitly within k_c.

B. Proposed Normalization Function Based Approach

In order to explicitly take the slot openings into account, we divide the stator into parallel slot segments (Figure 2) and express the stator tooth width in electric degrees

$$w_s = \pi \frac{D_s}{n} - w_{so} , \quad (5)$$

where D_s and n denote the inner diameter of the stator core and the number of stator slots, respectively. By applying this parallel-plate, instead of the cylindrical capacitor approximation, C_{rf} can then be written as

$$C_{rf} = \varepsilon_0 n l_s \frac{w_s}{d_{ag}} . \quad (6)$$

Similar to the case of a micro-strip capacitor over a ground plane, the electrode of the capacitor on the rotor side is wider

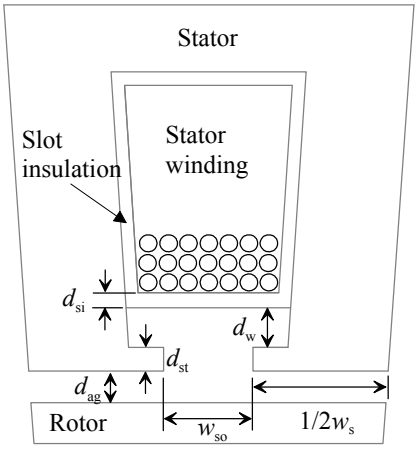

Figure 2. Schematic of a stator slot segment showing the parameters used in the modelling.

than the one on the stator side. Hence, the slot openings increase the total capacitance, when compared with the value of a parallel-plate capacitor with homogeneously distributed electric field, see Figure 3 and Figure 4. Thus, we amend the parallel-plate capacitor approximation to better describe this nonhomogeneous distribution of the electric field as follows:

The situation resembles the evaluation of distributed capacitances of a micro-strip transmission line typically used for

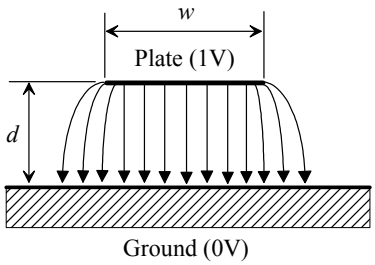

Figure 3. Micro-strip capacitor over the ground plane and associated electric field; the plate ends increase the total capacitance when compared with an ideal parallel-plate capacitor with homogenously distributed electric field.

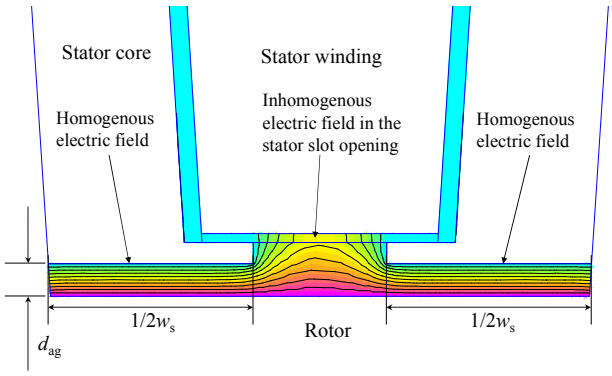

Figure 4. Electric field between the rotor and the stator frame as determined by the finite element method (electrostatic analysis, realized with Finite Element Methods Magnetics, [13]). The electric field is homogeneously distributed below the stator teeth and non-homogenously below the stator slot openings.

high-frequency signaling on printed circuit boards. An established, yet simple method to estimate the transmission line parameters consists in modeling the total capacitance C as sum of the plate capacitances C_y and the so called fringing capacitance C_f [14], which is the contribution of the plate ends to the total capacitance. With this assumption we express the normalized rotor-to-frame capacitance, $C_{rf,N}$, analytically,

$$C_{rf,N} = C_{rf}\left(1 + k_{rf}\right), \tag{7}$$

where k_{rf} is a function of the ratio between the machine air gap d_{ag} and the stator slot width w_s

$$k_{rf} = f\left(\frac{d_{ag}}{w_s}\right), \tag{8}$$

and is hence dimensionless.

Our claim is that the function k_{rf} can be estimated, e.g., by an extensive parameter study using numerical analysis, such as the finite element method. Evidently, the range of the parameters studied has to be "sufficiently" large, and care has to be taken when the results are applied to geometries not covered therein.

IV. Stator-Winding-to-Frame Capacitance Computation

A. Previously Proposed Approach

The stator-winding-to-rotor capacitance C_{wr} is formed between the stator windings in the slots and the rotor surface. It is much smaller than the rotor-to-frame capacitance C_{rf}, see Section II and (2). According to [15] and [16], the stator end winding also contributes to C_{wr}. Especially, in small induction machines, such as the off-the-shelf air-cooled 1.5 kW machine studied in [16], the effect of the end-winding on C_{wr} was found to be significant. We explain this by the relatively short stator stack compared to the end-winding as well as the short distance from the end-winding to the rotor end ring. As a result, this coupling and hence its contribution may not necessarily be as large in the case of larger machines.

A method to estimate C_{wr} based on the machine design parameters is presented in [10]. It assumes that each stator slot forms a parallel plate capacitor with the rotor surface, with a plate width of w_s and length l_s (Figure 2). The distance between the plates comprises the air gap distance d_{ag}, the stator tooth tip thickness d_{st}, the distance from the stator-slot to the winding d_w, and the slot insulation thickness d_{si} (Figure 2), thereby forming a series connection of capacitors with different relative permittivities ε_r. C_{wr} is then given by

$$C_{wr} = \varepsilon_0 n l_s \frac{w_{so}}{d_{ag} + \frac{d_{st}}{\varepsilon_{r,st}} + \frac{d_w}{\varepsilon_{r,w}} + \frac{d_{si}}{\varepsilon_{r,si}}}. \tag{9}$$

The proposed pure plate capacitor approach may overestimate the capacitance [16]. This is (again) explained by the inhomogeneous electric field distribution between the stator winding and the rotor, see also Figure 5.

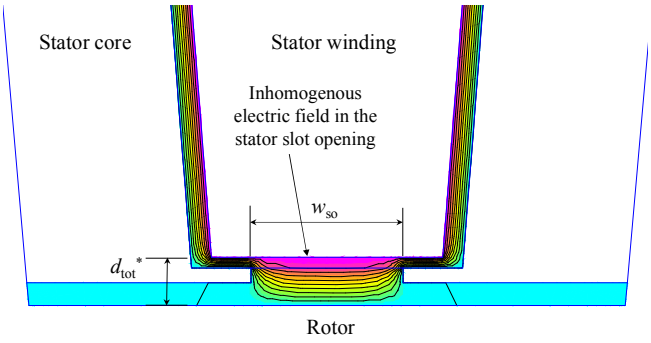

Figure 5. Inhomogeneous electric field distribution between the stator slot opening and the rotor as determined by the finite element method (electrostatic analysis, realized with Finite Element Methods Magnetics, [13]).

B. *Proposed Normalization Function Based Approach*

The authors of [17] remark that the electric field distribution in the stator slot opening is inhomogeneous due to complex geometrical design, and thus use of an FEM model for the calculation of the capacitance, already as a part of the machine design, is proposed.

The traditional parallel-plate capacitor approach has a low number of parameters that are readily available as part of the machine design process and provide a fairly explicit relationship between these and the computed capacitance. The authors of [18] proposed to consider the inhomogeneous field of a parallel-plate capacitor with a long distance d between the electrodes compared to their width w by normalizing the parallel-plate approximation by an adjustment coefficient k_{wr}. This coefficient is a function of the aspect ratio b,

$$b = \frac{d}{w} \tag{10}$$

and is derived from numerical computations using the boundary element method. We propose to use a similar dimensionless adjustment function k_{wr} to calculate the normalized stator-winding-to-rotor capacitance $C_{wr,N}$ based on the parallel-plate capacitor approximation of (9). It is defined as

$$C_{wr,N} = k_{wr} C_{wr}\text{, with} \tag{11}$$

$$k_{wr} = f\left(\frac{d_{tot}}{w_s}\right) \text{ and} \tag{12}$$

$$d_{tot} = d_{ag} + \frac{d_{st}}{\varepsilon_{r,st}} + \frac{d_w}{\varepsilon_{r,w}} + \frac{d_{si}}{\varepsilon_{r,si}}, \tag{13}$$

where d_{tot} denotes the effective distance between the electrodes in the parallel-plate capacitor.

Here again, our claim is that the function k_{wr} can be estimated, e.g., by an extensive parameter study using numerical analysis.

V. Determination of the Normalization Functions

Simplified electrostatic FEM models of the stator slot segments for two general purpose three-phase, four-pole, delta connected induction machines were developed. The first, M15kW, was a 15 kW with a shaft height of 160 mm, and the second, M37kW, a 37 kW machine with a shaft height of 225 mm. These machines were also selected for the experimental investigations and are further described below (Section VI, Table I shows the parameters.). These models comprise the original slot segment and the rotor surface, and are considered as reference models (Figure 5).

A. *Numerical Computation of the Normalized Capacitances $C_{wr,N}$ and $C_{rf,N}$*

The normalized rotor-to-frame and stator-winding-to-rotor capacitances are determined via FEM models as follows: First, a potential of 1 V is connected to the stator winding, while both the stator and the rotor are connected to a potential of 0 V. The resulting total charge of Q_1 is retrieved and the resulting capacitance C_1 calculated as

$$C_1 = \frac{Q_1}{1\text{V}}. \tag{14}$$

Next, the rotor is removed in the model, and the same procedure to calculate the total capacitance is repeated again to retrieve C_2. Finally, the normalized capacitance for $C_{wr,N}$ is given by

$$C_{wr,N} = n(C_1 - C_2). \tag{15}$$

In analogy, the normalized rotor to frame capacitance $C_{wr,N}$ is determined as follows: The rotor is connected to a potential of 1 V and the stator to 0 V. This time, the stator winding is removed in the FEM-model. Again the total charge and the resulting capacitance C_3 are computed and $C_{wr,N}$ is determined as

$$C_{rf,N} = nC_3. \tag{16}$$

Next, extensive parameter studies on the machine air gap d_{ag}, the stator-slot-to-winding distance d_w, and the stator slot opening width w_{so} were carried out, using numerical analysis. The stator tooth tip thickness d_{st} was kept constant, since preliminary FEM investigations had shown that varying this parameter almost has the same effect on the stator-winding-to-rotor capacitance as simply adjusting the distance d_w.

B. *Derivation of the Normalization Functions k_{rf} and k_{wr}*

For all the different scenarios, the values of C_{rf} and C_{wr} were calculated analytically from (6) and (9) respectively. The dependency between the normalized and analytically computed rotor-to-frame capacitances as a function of d_{ag}/w_s are illustrated in Figure 6, indicating a rather linear relationship. By employing the least mean squares (LMS) algorithm for a linear curve an empirical expression for the correction coefficient k_{rf} is derived,

$$k_{rf} = 2.3\frac{d_{ag}}{w_s}. \tag{17}$$

The correlation of this linear fitting is $R^2 = 0.87$.

The corresponding results for the ratios between the normalized stator-winding-to-rotor capacitance $C_{wr,N}/C_{wr}$ as a function of d_{tot}/w_{so} are shown in Figure 7, indicating a rather

exponential relationship.

Applying LMS again, we derive the following expression for the correction coefficient k_{wr}

$$k_{wr} = 1.194\mathrm{e}^{-2.81 d_{tot}/w_{so}} . \quad (18)$$

Here, the correlation of fitting is $R^2 = 0.99$.

The results shown in Figure 6 and 7 indicate that the same dimensionless normalization functions seem to be applicable, at least, for both of the investigated induction machines M15kW and M37kW and their stator slot segment design variants. Evidently, further research on further machines will increase the confidence into the generic nature of the normalization functions (8) and (12) as well as the correction coefficients presented in (17) and (18).

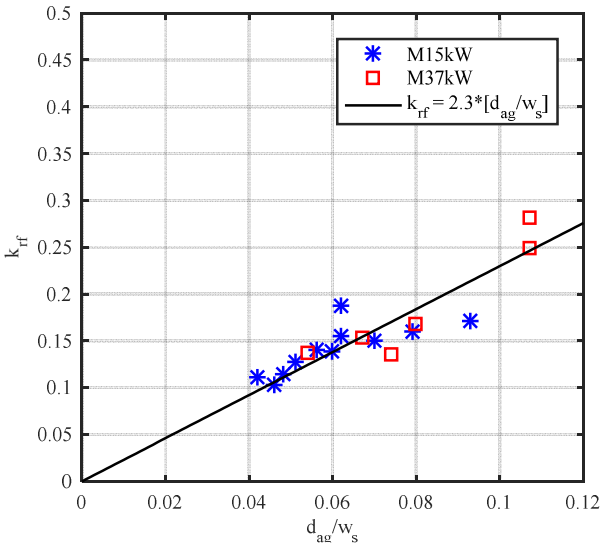

Figure 6. Numerically determined normalization coefficients k_{rw} for the parallel-plate capacitor approximation as a function of d_{tot}/w_{tot} for different ratios d_{tot}/w_{tot} of the two example case induction machine M15kW and M37kW.

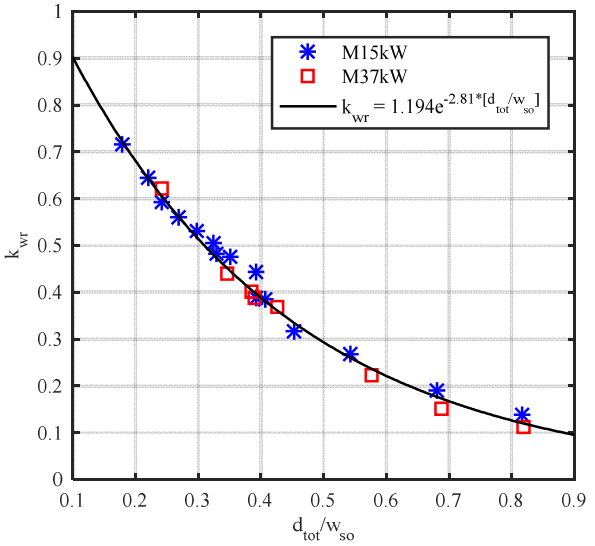

Figure 7. Numerically determined adjustment coefficients k_{wr} for the parallel-plate capacitor approximation as a function of d_{tot}/w_{tot} for different ratios d_{tot}/w_{tot} of the two example case induction machine M15kW and M37kW.

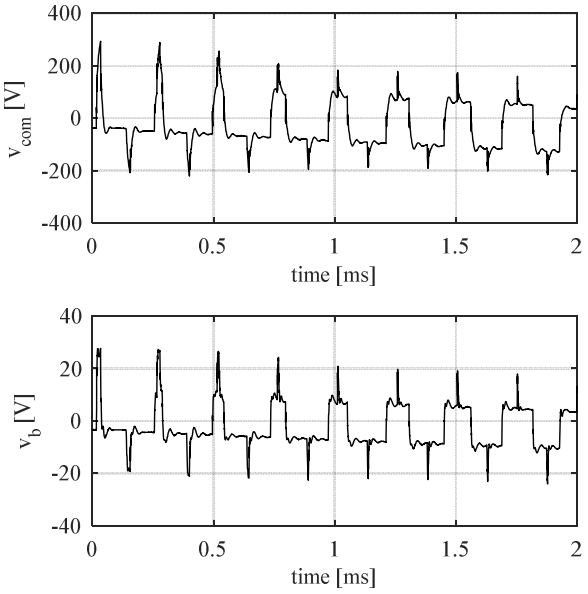

Figure 8. M15kW fed with a two-level frequency converter with 50 Hz supply frequency. Top: common-mode voltage measured at the stator terminals, bottom: measured voltage across the bearing. From these measurements, a BVR of 8.4 % is computed.

VI. Experimental Investigations

For both example case machines, M15kW and M37kW, first, the total rotor-to-stator-frame capacitances were measured with a Keysight U1733C handheld LCR meter using an excitation frequency of 1 kHz. Next, both machines were driven with a frequency converter at nominal speed, while the voltages across the bearings and the common mode voltage at the stator terminals were measured. For these, a Rohde & Schwartz RTO 1014 oscilloscope, along with Rohde & Schwartz differential voltage probes RT-ZD01 and an artificial star point made of three 1 MΩ resistors were used.

The BVRs were determined from the measured common mode and bearing voltages (Figure 8). Furthermore, the stator-winding-to-frame capacitances C_{wr} were computed from (1), along with the measured total rotor-to-frame capacitances C_{rf} and estimates of the bearing capacitances C_b. The machine parameters, as well as the different measured and estimated quantities are shown in TABLE I. Considering the geometries of the machine winding overhangs, we approximate that the capacitance between the winding overhangs and the rotor is (10-20) pF for both machines (e.g., M37kW shown in Figure 9). It is between 5 and 20 % of their total stator-winding-to-rotor capacitances, what is well in line with the values presented in [15] and [16].

For both investigated machines, based on machine design data, the proposed normalization method gives slightly lower values than the experimentally determined ones, both for C_{wr}

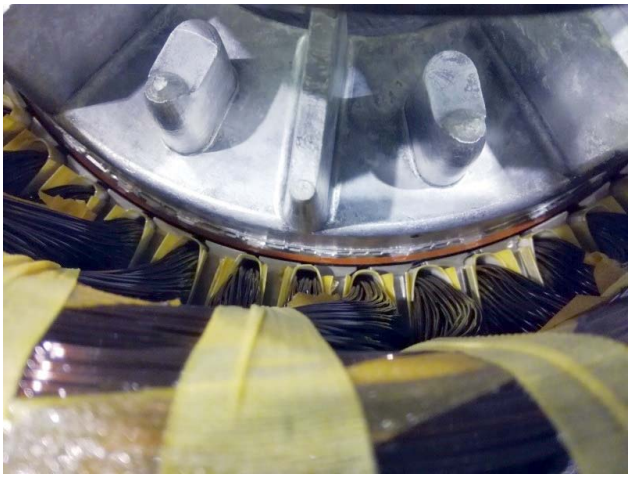

Figure 9. Non-drive-end of the general purpose three-phase, four-pole, delta connected 37 kW, 225 mm shaft height induction machine used for the experimental investigations**.** The winding overhang increases the total winding-to-rotor capacitance. With this machine, based on geometry and measured dimension, the additional capacitance is estimated to be 10-20 pF.

and $C_{rf,}$ see TABLE I. For M15kW, the estimated winding-to-rotor capacitance C_{wr} (172 pF + 15 pF = 187 pF) is 6.5 % smaller than the measured one (200 pF), the measured rotor-to-frame capacitance C_{rf} is 10 % smaller that the measured one (1890 pF versus 2100 pF). For M37kW, the differences are -20 % (78 pF + 15 pF = 93 pF versus 115 pF) and -9 % (1280 pF versus 1400 pF), respectively. A higher accuracy would certainly be desirable, and more research may identify the contributions to the capacitance not considered so far. However, the degree to which the capacitances are predicted is acceptable, and it is well in line with other approaches of similar complexity, and additionally easily applicable, including for the purpose of straightforward parameter studies. The BVRs determined by the proposed normalization method differ by 2 % and by -19 % from the experimentally determined values, for M15kW and for M37kW, respectively.

VII. Conclusion

The so-called bearing-voltage-ratio BVR has been recognized as an important parameter to estimate the likeliness with which a given electric machine may suffer from electric discharge machining bearing currents. The two main parameters that affect the BVR, the stator-winding-to-rotor and rotor-to-frame capacitances, C_{wr} and C_{rf}, are mainly defined already during the machine design. We proposed a new approach to calculate these capacitances by use of the simple analytic parallel-place capacitor equation and generic normalization functions derived from extensive parameter studies and electrostatic numerical analysis. The final expressions not only allow relatively accurately predicting the stator-winding-to-rotor and rotor-to-frame capacitances, but they are also easily applicable, allowing, for example, easily studying the sensitivity of the BVR towards changes of the different stator slot parameters.

TABLE I. Design data, measured, estimated and calculated parameters of the test machines.

	M15kW	**M37kW**
Design parameters		
Power [kW]	15	37
Pole number	4	4
Shaft height [mm]	160	225
Bearing types (DE/NDE)	6309/6208 C3, hybrid	6313/6213 C3
Number of stator slots n	36	48
Air gap d_{ag} [mm]	0.55	0.93
Stator inner diameter D_s [mm]	165	235
Stator core length l_s [mm]	270	205
Measured capacitances and BVRs		
Total rotor-to-frame capacitance $C_{rf,tot} = C_{rf} + C_{b,DE} + C_{b,NDE}$ [pF]	2200	3600
Bearing capacitances $C_{b,DE}+C_{b,NDE}$ [pF] (estimated)	50	2200
Rotor-to-frame capacitance C_{rf} [pF]	2100	1400
Bearing-voltage-ratio BVR [%]	8.4	3.1
Stator-winding-to-rotor capacitance $C_{wr} = BVR \cdot C_{rf,tot}/(1\text{-}BVR)$ [pF]	200	115
Estimated rotor-to-frame and stator-winding-to-rotor capacitances according to (6) and (9)		
C_{rf} [pF]	1680	1090
C_{wr} [pF]	319	205
BVR [%], according to (1)	15.6	5.9
C_{rf} and C_{wr} adjusted with the correction coefficients k_{rf} and k_{wr}		
$C_{rf,N}$ [pF]	1890	1280
$C_{wr,N}$ [pF]	172	78
$C_{wr,end}$ [pF] (estimated)	10-20	10-20
BVR [%], according to (1)	8.6	2.5
Differences between the computed and the measured values		
C_{rf}	- 10 %	- 9 %
C_{wr}	- 6.5 %	- 20 %
BVR	2 %	- 19 %

References

[1] S. Chen, T. A. Lipo, and D. Fitzgerald, "Modelling of bearing currents ininverter drives," *IEEE Trans. Ind. Appl.*, vol. 32, no. 6, pp. 1365–1370, Nov./Dec. 1996.

[2] J. Erdman, R. Kerkman, and D. Schlegel, "Effect of PWM inverters on AC motor bearing currents and shaft voltages," *IEEE Trans. Ind. Appl.*,vol. 32, no. 2, pp. 250–259, Mar./Apr. 1996.

[3] D. Busse, J. Erdman, R. Kerkman, D. Schlegel, and G. Skibinski, "The effect of PWM voltage source inverters on the mechanical performance of rolling bearings," *IEEE Trans. Ind. Appl.*, vol. 33, no. 2, pp. 567–576, Mar./Apr. 1997.

[4] D. Busse, J. Erdman, R. Kerkman, and D. Schlegel, "Bearing currents and their relationship to PWM drives," *IEEE Trans. Power Electron.*, vol. 12, no. 2, pp. 243–252, Mar. 1997.

[5] D. Busse, J. Erdman, R.J. Kerkman, D.Schlegel, G. Skibinski, "System Electrical Parameters an Their Effects on Bearing Currents", *IEEE Transactions Ind. Appl*. Vol. 33, No. 2, March/April 1997, pp. 577-584.

[6] S. Bell, T. J. Cookson, S. A. Cope, R. A. Epperly, A. Fischer, D.W. Schlegel, and G. L. Skibinski, "Experience with variable-frequency drives and motor bearing reliability," *IEEE Trans. Ind. Appl.*, vol. 37, no. 5, pp. 1438–1446, Sep./Oct. 1998.

[7] E. Wittek, M. Kriese, H. Tischmacher, S. Gattermann, B. Ponick, G. Poll, "Capacitances and lubricant film thicknesses of motor bearings under different operating conditions", in *ICEM 2010*, 6-8 Sept. 2010, Rome, Italy.

[8] O. Magdun, A. Binder, "Calculation of Roller and Ball Bearing Capacitances and Prediction of EDM Currents", in *IECON'09*, 3-5 Nov. 2009. pp. 1051-1056.

[9] V. Niskanen, A. Muetze, J. Ahola. Study on Bearing Impedance Properties at Several Hundred Kilohertz for Different Electric Machine Operating Parameters, *IEEE Trans. Ind. Appl.*, 50(5), 2014, pp. 3438–3447.

[10] A. Muetze, A. Binder, "Calculation of Motor Capacitances for Prediction of the Voltage Across the Bearings in Machines of Inverter-Based Drive Systems, *IEEE Trans. Ind. Appl.*, Vol. 43, No. 3, May/June 2007, pp. 665-672.

[11] O. Magdun, A. Binder, "High-Frequency Induction Machine Modeling for Common Mode Current and Bearing Voltage Calculation", *IEEE Trans. Ind. Appl.*, Vol. 50, No. 3, May/June 2014.

[12] O. Magdun, Y. Gemeinder, A. Binder, K. Reis, "Calculation of Bearing and Common-Mode Voltages for the Prediction of Bearing Failures Caused by EDM Currents", in *SDEMPED 2011*, 5-8 Sept. 2011, Bologna, Italy, pp. 462-467.

[13] K.B. Baltzis, "The finite element method magnetics (FEMM) freeware package: May it serve as an educational tool in teaching electromagnetics?", *Educ. Inf. Technol*. (2010), 15, pp. 19-36.

[14] H. Nishiyama, M. Nakamura, "Capacitance of a Strip Capacitor", *IEEE Transactions on Components, Hybrids, and Manufacturing Technology*, Vol. 13, No. 2, June 1990, pp. 417-423.

[15] J. Adabi, F. Zare, A. Ghosh, R.D. Lorenz, "Calculations of capacitive couplings induction generators to analyse shaft voltage, *IET Power Electron.*, 2010, Vol. 3, Iss. 3, pp. 379-390.

[16] O. Magdun, Y. Gemeinder, A. Binder, "Prevention of Harmful EDM Currents in Inverter-fed AC Machines by Use of Electrostatic Shields in the Stator Winding Overhang, in *IECON 2010*, 7-10 Nov. 2010, Glendale, AZ, USA, pp. 962-967.

[17] M. Kriese, E. Wittek, S. Gatterman, H. Tischmacher, G. Poll, B. Ponick, "Prediction of Motor Bering Currents for Converter Operation", in *ICEM 2010*, 6-8 Sept. 2010, Rome, Italy.

[18] H. Nishiyama, M. Nakamura, "Form and Capacitance of Parallel Plate Capacitors", *IEEE Transactions on Components, Packaging, and Manufacturing Technology* – Part A, Vol. 17, No. 3, September 1994, pp. 477-484.